# Cloud-Edge Cooperative Model and Closed-Loop Control Strategy for the Price Response of Large-Scale Air Conditioners Considering Data Packet Dropouts

Aihua Jiang, Hua Wei, Jun Deng, and Hua Qin

***Abstract*—The price-based demand response has been considered one of the most effective ways to reduce the peak demand of power grids. However, it is possible to form a new rebound critical peak to threaten the grid stability and economic operation when large-scale loads respond to the price signal simultaneously. Based on the Internet of Things (IoT), this paper proposes a cloud-edge coordination (CEC) automatic control strategy to enable interaction and cooperation among the power grid and massive individual air conditioners (ACs) and eliminate the grid rebound critical peak of the synchro-response. Edge computing actively provides optional cooperation electricity plans, migrates computationally intensive tasks from the cloud and guarantees the privacy of users. Considering the unreliability of network transmission, data packet dropouts (/or delays and even downtime) are inevitable and usually random in the transmission, and a dual-feedback closed-loop control is first proposed in this paper. Finally, the effectiveness of the optimized closed-loop control strategy is verified by simulation cases.**

***Index Terms*—Internet of Things, cloud-edge cooperative, rebound effect, large-scale heterogeneous air conditioning, cooperative game, price-based demand response.**

## NOMENCLATURE

*Abbreviations*

| | |
|---|---|
| PBDR | Price-based demand response |
| ACs | Air conditioners |
| CEC | Cloud-edge coordination |
| MPC | Model predictive control |
| DSM | Demand-side management |
| DP | Disagreement point |
| AP | Agreement point |
| NBS | Nash bargaining solution |
| TOU | Time of use |
| IoT | Internet of Things. |

*Sets and Indices*

| | |
|---|---|
| $\mathbb{I}=\{1,\ldots,i,\ldots,N\}$ | Set of the ACs, indexed by $i$; |
| $\mathbb{T}=\{0,1,\ldots t,\ldots\}$ | Set of the control time step, indexed by $t$; |
| $\mathbb{K}=\{0,\ldots,k,\ldots,K_T-1\}$ | Set of the prediction horizon, indexed by $k$; |

*Variables*

| | |
|---|---|
| $TM_i^{\text{in}}(t)$ | Indoor control temperature in the time step $t$ by $AC_i$, (°C) |
| $P_i(t)$ | $P_i(t)=\{P_i(t+0)\|_t,\ldots,P_i(t+k)\|_t,\ldots,P_i(t+K-1)\|_t\}$ Average cooling power consumed by the $AC_i$ in the time step $t$, (kW) |
| $P^{\text{peak}}(t+k^{\text{P}}\|_t)$ | The critical peak of the grid in the prediction horizon, in time step $t$, (kW) |
| $P_{i,l}(t+k\|_t)$ | The predicted power at slot $t+k$ in control period $t$ by $AC_i$ in the $l$-$th$ round of negotiations, (kW) |
| $TM_i^{\text{in}}(t+k\|_t)$ | The indoor temperature at prediction $t+k$ in time step $t$, (°C) |
| $P_l^{\text{DP}}(t+k_l^{\text{DP}}\|_t)$ | DP of the total grid power for the $l$-$th$ bargaining happening at prediction slot $t+k_l^{\text{DP}}$ in control step $t$; |
| $\zeta(t),\lambda(t),\gamma(t)\in\{0,1\}$ | Bernoulli stochastic variables. 1 stands for data packet delivery success, and 0 stands for packet delivery failure. |
| $\mu_{i,l}(t)\in\{0,1\}$ | Cooperation decision variable; 1 stands for cooperation, and 0 stands for noncooperation; |
| $P_i^{\text{act}}(t)$ | Execution volume of the $i$-actuator at $t$; |

*Parameters*

| | |
|---|---|
| $\tau$ | Sampling period; |
| $\alpha_i$ | Thermal characteristics of the thermal mass; |
| $\beta_i$ | Energy efficiency coefficient; |
| $b_i$ | The weighted coefficient for user comfort and electricity cost; |

Manuscript received August 21, 2019; revised December 5, 2019, January 24, 2020, and March 8, 2020; accepted March 31, 2020. Date of publication May 19, 2020; date of current version August 21, 2020. This work was supported by the National Science Foundation of China under Grant 51667004. Paper no. TSG-01212-2019. *(Corresponding author: Aihua Jiang.)*

Aihua Jiang and Hua Wei are with the Guangxi Key Laboratory of Power System Optimization and Energy Technology, Guangxi University, Nanning 530004, China (e-mail: 1261153682@qq.com).

Jun Deng is with the State Grid Shaanxi Electric Power Research Institute, Xi'an 710000, China.

Hua Qin is with the School of Computer, Electronics and information, Guangxi University, Nanning 530004, China.

Color versions of one or more of the figures in this article are available online at http://ieeexplore.ieee.org.

Digital Object Identifier 10.1109/TSG.2020.2985741

| | |
|---|---|
| $\bar{P}_i$ | Rated power of the $AC_i$; |
| $P^{g'}(t)$ | Baseload (kW) in a control period *t;* |
| $TM_i^{\text{out}}(t)$ | Outdoor ambient temperature (°C) at *t;* |
| $TM_i^{\text{comf}}$ | The most satisfactory user-defined temperature, (°C); |
| $C(t+k\|_t)$ | Prediction of the electricity price at prediction slot *t+k* in control period *t*; |
| $\underline{TM}_i^{\text{comf}}$ | Lower limits of the user's tolerable temperature (°C); |
| $\overline{TM}_i^{\text{comf}}$ | Upper limits of the user's tolerable temperature (°C); |
| $w_i(t)$ | Random disturbance for $AC_i$ in *t.* |

## I. Introduction

### A. Background and Motivation

REDUCING the peak load of the power grid can bring tremendous economic benefits. The demand response (DR) has been widely recognized as an important approach to reduce the peak load of power systems. DR programs are generally classified into two categories: incentive-based demand response (IBDR) and price-based demand response (PBDR) [1], [2]. IBDR programs are dispatchable, but PBDR programs, such as real-time pricing (RTP), time of use (TOU) and critical peak pricing (CPP) programs, are nondispatchable [3]. Because the user decides whether or not to respond to the price signal, it is difficult to dispatch according to the grid variety. When many customers respond to the same time-varying price signal, there is a potentially significant risk that all the loads may shift from peak time to non-peak time at the same time. In this case, although the objective of the DR program is to reduce demand during high price periods, an unexpected peak demand called a rebound peak may occur. This effect may lead to an even higher demand peak than that which the DR program tried to avoid in the first place, which may threaten grid stability [4], [5]. This phenomenon has been observed in many pilot projects, such as the Californian pilot study of TOU and CPP [6].

The power demand of residential air conditioners (ACs) continues to increase, especially during the summer. According to statistics, AC loads account for approximately 35%, 33%, and 40% of electricity consumption during peak summer hours in many load centers in China, Spain, and India, respectively [5]. Reducing the power demand of ACs during peak hours via DR has become an important task for the management of AC loads. However, as reviewed in [7], ACs typically have small, time-varying, and geographically dispersed loads. The operation of each AC depends on its task specifications (e.g., start time, task duration, most satisfactory temperature, tolerable temperature range, and cost satisfaction), which are not known a priori until the user decides to turn an appliance on. Given these features of ACs, it is difficult to handle system-wide dispatch for the grid, especially for real-time operation [8].

Eliminating the rebound critical peak in the face of the same time-varying price signal without the intervention of utility operators is a valuable research topic. With the advent of the Internet of Things (IoT), can we solve the peak-rebound problem based on the cloud? The challenges we still face include massive data storage, control decisions, computational complexity due to uncertainty and the unreliability of network transmission.

*1) Literature Survey:* Currently, two major types of AC control strategies for the DR program have been investigated. The first is based on an individual's response to prices or incentives [9], [10], [11], which is mainly aimed at reducing the power consumption of users and the cost, regardless of their impact on the power grid. Usually, each user only accounts for a very small portion of the total load, but the number of residential users is enormous, and thus, communication and supervision directly from the utility operator are difficult and costly [12]. To efficiently leverage the scale effect of small loads for the economic operation of power grids, aggregation-based direct load control has become the mainstream of research on the application of large-scale small loads for the DR program [13], [14]. Reference [15] presented an algorithm for maximum load reduction based on the aggregated power demand of a group of heating, ventilating and air conditioning (HVAC) units. Reference [16] presented a direct load control strategy based on the aggregation model for operating reserves and actively responding. Reference [17] presented a real-time trading framework for distribution networks in which an aggregator is identified as a broker by contracting with individual demands and dealing with the distribution company. Reference [18] formulated the AC control problem as an optimization problem to be solved by the aggregated model in a model predictive control framework for power balancing. Reference [19] proposed a hierarchical approach with a three-level control framework for reliable scheduling and the provision of frequency reserves by aggregating commercial buildings. In [20], Schlueter *et al.* discussed data-driven clustering for the optimally efficient creation of thermal microgrids using existing building stocks.

In the aggregation-based strategy, the peak shift problem caused by the aggregated AC load DR has been noticed and addressed by some researchers. For example, [28] proposed a concept to achieve better control of the DR rebound by coordinating different groups of ACs. However, a mathematical model was missing to determine the coordination process among various AC groups. Reference [29] proposed a coordinating mechanism in a neighborhood area through the interactions between the energy management actions of multiple households to reduce the rebound peaks. Reference [30] proposed an optimal sequential dispatch strategy of ACs to mitigate the rebound effect based on the aggregation model.

Coordinated energy management based on a multi-agent control system is studied in either centralized or decentralized manners [21], [22], [23]. Although these studies proposed various coordination mechanisms with a focus on different aspects, they tend to model entities (smart homes, aggregators, and utility) as agents [21]. For example, [24] gives a typical multi-agent framework. It includes the auctioneer agent, concentrator agents, and device agents. The device agent controls the cluster of loads. Some published papers are using the agent-based and game theory integrated method for the cooperation of the power grid and demand response resources. Such as [25]

propose a distributed energy demand scheduling approach based on multi-leader-follower game for Smart Building. Each building is represented by an agent. Reference [26] proposed a Population Games to foster s cooperation between DR participants for rapid convergence to expected aggregate load curtailment. Household demand is represented by an agent. Reference [27] proposed an approach that is modular and distributed by nature based on the Nash Bargaining Solution. The demand response agent is load aggregator in charge of providing DR services in the microgrid. Moreover, the results presented in these papers are based on only a small number of agent participants. With the increase of agents, solution calculation for the game will become more complex.

In the above aggregation-based strategy research, the model for controlling the ACs was formulated into an optimal scheduling problem. Moreover, all the above efforts are based on direct load control (a typical IBDR program), which may experience data availability and data privacy issues. Although the IBDR program is dispatchable, it is only executed during the release period for which the time and frequency are limited.

The PBDR program has a good guiding effect on daily load management and is a regular DR program. However, the response to price signals still faces nontrivial challenges; specifically, the load response of loads is nondispatchable. Because the response control was decided by users rather than the dispatcher, it is difficult to schedule according to the needs of the grid. As a result, large-scale load response price signals tend to simultaneously incur peak rebound. The impact of the rebound peak cannot be ignored. To the best of our knowledge, few research efforts have addressed this issue.

In our previous study [31], a distributed control strategy for reducing the lead-rebound peak caused by the PBDR program is presented. The objective of the system is decomposed into distributed AC controllers, and the final decision is made by the AC controller. Due to the limitations of the distributed algorithm, improving global performance is a challenge [32].

### B. Major Contributions

Based on the above research gaps, to improve the global performance of the grid with the development of the IoT, one cloud-based solution is to build a centralized and optimized coordination control strategy for the users and the power grid. In Section II, we discuss the cloud coordinated control model, which is based on multi-objective nonlinear programming. The computational complexity of the model will increase significantly as the size of the load increases, accompanied by the need for massive parameter storage. It is generally believed that the control strategy can achieve good global performance but is not practical in a large-scale system due to computational and storage requirements and the lack of error tolerance [32].

We propose a cloud-edge coordination (CEC) automatic control strategy based on cooperative game theory to enable interactions and cooperation among the power grid and numerous ACs. The key idea of the CEC strategy is to migrate computationally intensive tasks from the cloud to numerous edged devices. The cloud platform is only responsible for the negotiation and decision, while the edged devices are responsible for the parallel collaboration computing. The advantage is that cooperation computing of edge devices not only shares computing tasks but also guarantees users' privacy. We show that the proposed control strategy naturally leads to a distributed and parallel implementation, requiring only limited coordination with the cloud.

Our main contributions are summarized as follows:

1. A CEC automatic control strategy is proposed to enable interaction and cooperation among the power grid and massive individual ACs to eliminate the grid rebound critical peak of the synchro-response.
2. Edge computing actively provides optional cooperation electricity plans, greatly reduces the computational complexity and data storage of the cloud. Additionally, it guarantees the users' privacy.
3. A dual-feedback closed-loop control is first proposed to ensure the control stability and optimization in the paper, considering the unreliability of network transmission and the inevitability and randomness of data packet dropouts (or delays and even downtime) in the transmission.

### C. Organization of the Paper

The remainder of this paper is structured as follows. In Section II, we briefly describe the problem. In Section III, we introduce the fundamental concepts of cooperative game theory, which provides the foundation of our proposed CEC strategy. Subsequently, in Section IV, the control framework, model and information interaction of the CEC strategy are presented in detail. Section V presents two cases that validate the effectiveness and efficiency of our proposed method. Finally, in Section VI, we conclude our work.

## II. Problem Description

In this section, we simply describe the PBDR model of an AC, with the target of reducing critical peaks in power grids and establishing a centralized coordination model based on the cloud for ease of understanding and comparison.

### A. Individual Goals for AC Users

Each AC can have its own private model due to different building structures and AC types. It can be a first-order or second-order model or consider the occupancy of personnel. The general thermal model is employed in the paper to facilitate large-scale simulation because our focus is not on the AC model, but on the cooperation between users. An AC user can reduce charges and maintain comfort satisfaction by responding to electricity prices. The expectation model for $AC_i$ in the prediction horizon $\mathbb{K} = \{0, \ldots, k, \ldots K_T - 1\}$ is as

follows [9], [33]:

$$\begin{cases} \min \sum_{k=t}^{t+K_T-1} \Big[ \tau P_i(t+k|_t) C(t+k|_t) \\ \qquad + b_i \big( TM_i^{\text{in}}(t+k|_t) - TM_i^{\text{comf}} \big)^2 \Big]; \\ TM_i^{\text{in}}(t+1) = (1-\alpha_i) \big( TM_i^{\text{out}}(t+1) + \alpha_i TM_i^{\text{in}}(t) \\ \qquad - R_i \beta_i P_i(t)) + w_i(t); \\ \underline{TM}_i^{\text{comf}} \le TM_i^{\text{in}}(t) \le \overline{TM}_i^{\text{comf}}; \\ 0 \le P_i(t) \le \bar{P}_i \quad \forall t; \\ t \in \mathbb{T}; \quad k \in \mathbb{K}; \quad i \in \mathbb{I} \end{cases} \tag{1}$$

where $\min \sum_{k=t}^{t+K_T-1} [\tau P_i(t+k|_t) C(t+k|_t) + b_i (TM_i^{\text{in}}(t+k|_t) - TM_i^{\text{comf}})^2]$ is the user's expectation. Every user wants to minimize the amount spent and maintain a comfortable indoor temperature within the range of their own settings $[\underline{TM}_i^{\text{comf}}, \overline{TM}_i^{\text{comf}}]$. $TM_i^{\text{in}}(t+1) = (1-\alpha_i)(TM_i^{\text{out}}(t+1) + \alpha_i TM_i^{\text{in}}(t) - R_i \beta_i P_i(t)) + w_i(t)$is the physical model for $AC_i$ and can be understood as the average power consumed to maintain a level of indoor temperature in a given period.

### B. Grid Target

For the power grid, the expectation is to minimize the maximum power consumption (critical peak) of the grid. The objective can be written as

$$J^{\text{g}}(t) = \min \left( \max \left( \sum_{i=1}^{N} P_i(t+k|_t) + P^{\text{g}'}(t+k|_t) \right) \right) \tag{2}$$

The variable $P^{\text{peak}}(t+k_p|_t) = \max(\sum_{i=1}^{N} P_i(t+k|_t) + P^{\text{g}'}(t+k|_t))$, which is the maximum power of the grid in the prediction horizon $\mathbb{K} = \{0, \ldots, k, \ldots K_T - 1\}$, is introduced. Thus, (2) is converted into a solution for the following optimization problem:

$$\begin{cases} J^{\text{g}}(t) = \min P^{\text{peak}}\big(t+k_p|_t\big); \\ P^{\text{peak}}\big(t+k_p|_t\big) \ge P^{\text{g}'}(t+k|_t) + \sum_{i=1}^{N} P_i(t+k|_t). \end{cases} \tag{3}$$

### C. The Centralized Coordinated Control Model for the Cloud

To facilitate comparison, we write the centralized coordinate control model for the cloud that satisfies both user and grid requirements. The model can be written as follows:

$$\begin{cases} J^{\text{g}}(t) = \min P^{\text{peak}}\big(t+k_p|_t\big) \\ J_i = \min \sum_{k=t}^{t+K_T-1} \Big[ \tau C(t+k|_t) P_i(t+k|_t) \\ \qquad + b_i \big( TM_i^{\text{in}}(t+k|_t) - TM_i^{\text{comf}} \big)^2 \Big] \\ TM_i^{\text{in}}(t+1) = \alpha_i TM_i^{\text{in}}(t) + (1-\alpha_i) \\ \qquad \times \big( TM_i^{\text{out}}(t+1) - R_i \beta_i P_i(t) \big) + w_i(t); \\ \underline{TM}_i^{\text{comf}} \le TM_i^{\text{in}}(t) \le \overline{TM}_i^{\text{comf}} \\ 0 \le P_i(t) \le \bar{P}_i \quad \forall t \\ P^{\text{peak}}\big(t+k_p|_t\big) \ge P^{\text{g}}(t+k|_t) + \sum_{i=1}^{N} P_i(t+k|_t); \\ k \in \mathbb{K}; t \in \mathbb{T}; i \in \mathbb{I}; \end{cases} \tag{4}$$

Model (4) is a nonlinear multiobjective optimization problem. The number of variables increases greatly as the number of ACs increases. The complexity is discussed in Section IV-D.

## III. Fundamentals of Cooperative Game Theory

We briefly introduce the basic concepts of cooperative game theory, which provides the foundation of our proposed CEC strategy.

The basic component of game theory is a game, $G = \langle \mathbb{I}, \{\Omega_i\}_{i \in \mathbb{I}}, \{f_i\}_{i \in \mathbb{I}} \rangle$, where $\mathbb{I} = \{1, \ldots, N\}$ is the set of players, $\Omega_i$ is the nonempty set of feasible control actions for player i and $\Omega_i = \Omega_1 \times \cdots \times \Omega_N \to \mathbb{R}$. $f_i$ is the utility function (or objective function), which player $i$ wishes to maximize. In a cooperative game, players negotiate with each other before the game is played. If an agreement is reached, players act according to the agreement reached; otherwise, players act in a noncooperative way. Before we proceed, we need to introduce some terminology. An agreement point (AP) is any control action vector $u \in \Omega$ that is a possible outcome of the bargaining process. The concept of the disagreement point (DP) refers to the optimal result for the worst situation. A DP is an action vector $u \in \Omega$ that is expected to be the result of noncooperative play given a failure of the bargaining process (i.e., what will happen if players cannot come to an agreement). Clearly, the objective achieved by every player at any AP has to be at least as much as the objective achieved at the DP. A bargaining solution is a map that assigns a solution to a given cooperative game. The negotiation solution process of axiomatic bargaining game theory, as discussed by Nash in [34], [35] is presented below.

*Theorem:* Let $\Phi = \{f_i(u) | u \in \Omega\}$ be a convex maximizer utility, with a closed and upper bound $f_i^* \ge f_i^d$ as a subset of $\mathbb{R}^N$. Let $u^d$ be the DP. Let $f_i^d = f_i(u^d)$ be the utility of player $i$ achieved at the DP, let and $\Phi^d = \{\mathbf{f}(u) \in \Phi | \mathbf{f} \ge \mathbf{f}^d\}$ be the set of achievable utilities. Let $\mathbb{I} = \{1, \ldots, N | \exists \mathbf{f} \in \Phi^d, f_i > f_i^d\}$ be the set of players that can achieve a utility that is strictly greater than the disagreement objective. Then, the Nash Product (NP)$\mathbf{f}^* = \varphi(\Phi, \mathbf{f}^d)$ is the unique Nash bargaining solution (NBS):

$$\mathbf{f}^* = \arg \max_{\mathbf{f} \in \Phi^d} \prod_{i \in \mathbb{I}} \Big( f_i - f_i^d \Big) \tag{5}$$

The maximization problem (5) can be equivalently rewritten as

$$\mathbf{f}^* = \arg \max_{\mathbf{f} \in \Phi^d} \sum_{i \in \mathbb{I}} \log \Big( f_i - f_i^d \Big) \tag{6}$$

Based on cooperative game theory, the key idea of the CEC control strategy is that the cloud computing center only decides how to cooperate to reduce the critical peak, which corresponds to a negotiation to find the DP and AP in the game. In our problem, player $AC_i$ can reach an agreement as long as the comfort and expenses are met, but the grid as a player cannot come to an agreement until the critical peak of the grid is minimized. Thus, the critical peak point of the grid is the DP.

## IV. CEC Control Strategy

### A. A Schematic Overview

The massive individual ACs were connected to the Internet to cooperate with each other to reduce the power grid peak, as shown in Fig. 1. The AC device communicates with the

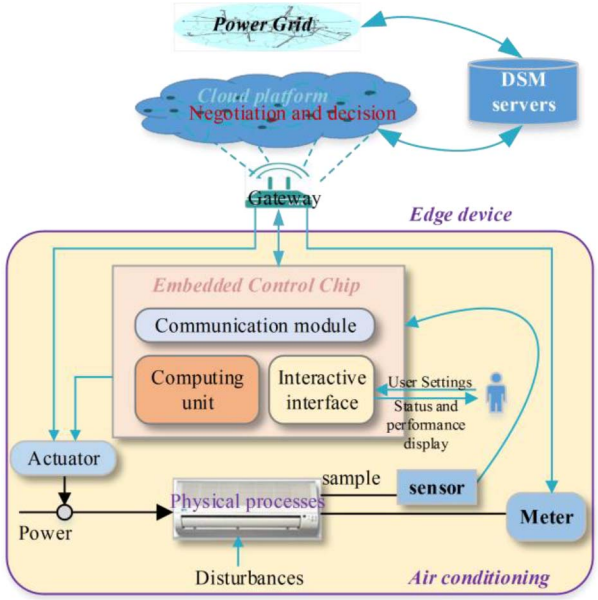


Fig. 1. Components and architecture for an edged AC device in IoT.

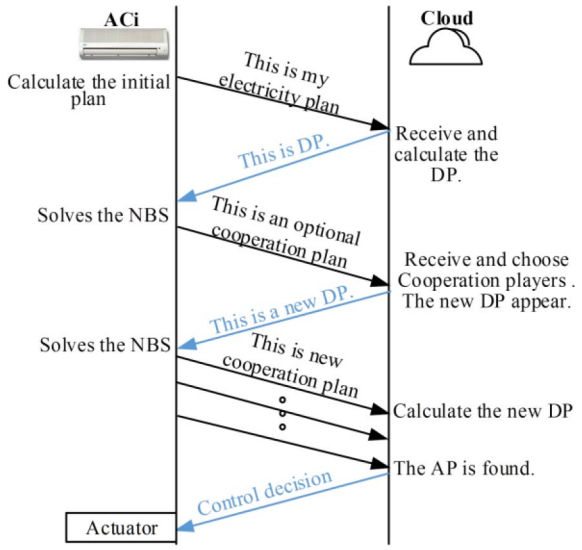


Fig. 2. A schematic overview.

cloud platform via the gateway. The cloud platform not only receives the information of each AC but also needs the grid real-time load and predicted load data from the demand-side management servers to make decisions.

The components and architecture for an edged AC device in the IoT are also shown in Fig. 1. The control components of the edged AC device consist of sensors, meters, an embedded control chip, and actuators. The embedded control chip contains an edge computing module, a wireless communication module, and a human-computer interaction module. The communication module receives information such as the indoor and outdoor temperatures from the sensor, the DP, and the weather forecast from the cloud.

In order to make the proposed method understandable, a schematic overview of the CEC strategy is shown in Fig. 2.

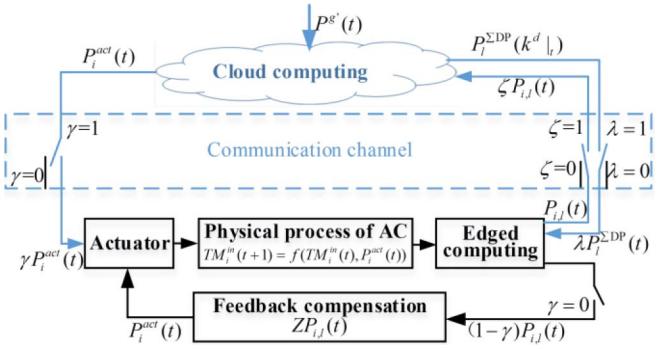


Fig. 3. The double feedback closed-loop control framework considering data packet dropouts.

Each AC can calculate the initial optimal electricity consumption plan in response to the price (without communication and cooperation, each AC will respond to the electricity price at the same time). The plan is sent to the cloud to calculate the grid critical peak (that is, the DP). Then, the DP is broadcast to every AC. According to cooperative game theory, each $AC_i$ independently solves the NBS (feasible cooperation plan), which reduces the power consumption at the time of the DP. Then, it is sent to the cloud for negotiation again. Each cooperation negotiation makes the critical peak lower than the last negotiation until the critical peak is no longer reduced. That is, the AP is found. We also assume that the device is networked. In networked systems, random delays and packet dropouts are unavoidable. Sometimes there will be downtime events [36], which means communication is completely interrupted. To guarantee the stability of the control, we design a dual-feedback closed-loop control structure based on model predictive control (MPC) [37].

The corresponding detailed control framework in a time step is shown in Fig. 3. The feasible power usage plan of $AC_i$ is to be solved by edged computing; it is then packaged and sent to the cloud platform. The cloud platform computes the DP. If the DP fails to reach the AP, the DP is packaged and broadcast to every AC. $AC_i$ receives the DP, resolves the feasible power usage plan and sends it to the cloud again. This process repeats until the cloud platform obtains the AP. According to MPC, only the first step is applied in the resulting control sequence. The first element of the AP, which is the decision control volume, is packaged and broadcast to the corresponding AC actuators. If the decision packet drops out, the local feedback will be executed. The packet dropout event is modeled as a Bernoulli stochastic variable $\zeta(t), \lambda(t), \gamma(t) \in \{0, 1\}$. 1 stands for packet delivery success, and 0 stands for delivery failure. The models, information interaction and data processing of the CEC strategy are introduced in the following subsection.

### B. The Models and Information Interaction

*1) Initialization for $AC_i$:* The control model for the independent response of $AC_i$ to the price is model (1), and the solution $P_i(t)$ is defined as the initial value for the bargaining.

Let $P_{i,0}^{\mathrm{NBS}}(t) = P_i(t)$; it is then packed and uploaded to the cloud.

*2) The Model for Communication Channel Packet Dropouts:* The channel missing packet event is modeled as a Bernoulli stochastic variable $\zeta(t), \lambda(t), \gamma(t) \in \{0, 1\}$. 1 stands for packet delivery success, and 0 stands for delivery failure.

$$\begin{aligned}&\mathrm{Prob}\{\zeta(t)=1\}=\sigma_\zeta;\mathrm{Prob}\{\zeta(t)=0\}=1-\sigma_\zeta\\&\mathrm{Prob}\{\lambda(t)=1\}=\sigma_\lambda;\mathrm{Prob}\{\lambda(t)=0\}=1-\sigma_\lambda\\&\mathrm{Prob}\{\gamma(t)=1\}=\sigma_\gamma;\mathrm{Prob}\{\gamma(t)=0\}=1-\sigma_\gamma\end{aligned}$$

where $\sigma$ is a known positive scalar. The Bernoulli stochastic variables are independent variables that are not connected. For example, $\mathrm{AC}_i$ uploads a packet to the cloud, $\mathrm{Prob}\{\zeta_{\mathrm{AC}1,l}(t)=1\}=0.99$ means that the probability of correct packet delivery to the cloud platform is 99% and the probability of packet dropout is 1%.

*3) DP Initialization for Cloud Computing:* In the cloud platform, let us define the available information set $\mathbb{I}_{t,0} = \{i, P_{i,0}^{\mathrm{NBS}}(t)|_{\zeta_{i,0}(t)=1}\}$ according to the packets received from the different ACs. In addition to another message $P^{g'}(t)$ received from the demand-side management (DSM) server, the DP initialization model is

$$\begin{cases}\min P_0^{\mathrm{DP}}\big(t+k_0^{\mathrm{DP}}|_t\big)\\ P_0^{\mathrm{DP}}\big(t+k_0^{\mathrm{DP}}|_t\big)\geq P^{g'}(t+k|_t)\\ \quad+\sum_{i=1}^{N}\zeta_{i,0}(t+k|_t)P_{i,0}^{\mathrm{NBS}}(t+k|_t)\\ k\in\mathbb{K};\,t\in\mathbb{T};\,i\in\mathbb{I}_{t,0}\end{cases}\tag{7}$$

$P_0^{\mathrm{DP}}(t+k_0^{\mathrm{DP}}|_t)$ is packed and broadcast to every AC device.

*4) Cooperation Model for Edge Computing:* If $\lambda_{i,l}=1$, the edged $AC_i$ device received the DP packet successfully from the cloud. The cooperation rule is designed as follows: the interests of the users are guaranteed (the cost is not increased, and the indoor temperature is within the tolerable range); and the interest of the grid is the minimum power peak. According to (6) in Section III, the cooperation agreement is to keep the electricity charge unchanged within the allowable comfort range, and the cooperation model can be written as

$$\begin{cases}\max\log\Big[\lambda_{i,l}(t)P_{l-1}^{DP}\big(t+k_{l-1}^{DP}|_t\big)-P_{i,l}^{\mathrm{NBS}}\big(t+k_l^{\mathrm{DP}}|_t\big)\Big];\\ \min\sum_{k=t}^{t+K_T-1}\Big[\tau P_{i,l}^{\mathrm{NBS}}(t+k|_t)\,C(t+k|_t)\\ \qquad+b_i\big(TM_i^{\mathrm{in}}(t+k|_t)-TM_i^{\mathrm{comf}}\big)^2\Big];\\ P_{l-1}^{DP}\big(t+k_{l-1}^{DP}|_t\big)\geq P_{i,l}^{\mathrm{NBS}}\big(t+k_l^{\mathrm{DP}}|_t\big);\\ TM_i^{\mathrm{in}}(t+1)=(1-\alpha_i)\Big(TM_i^{\mathrm{out}}(t+1)+\alpha_i TM_i^{\mathrm{in}}(t)\\ \qquad-R_i\beta_i P_{i,l}^{\mathrm{NBS}}(t)\Big)+w_i(t);\\ \sum_{k=t}^{t+K_T-1}\Big[\tau P_{i,l}^{\mathrm{NBS}}(t+k|_t)\,C(t+k|_t)\\ \qquad\leq\sum_{k=t}^{t+K_T-1}\Big[\tau P_{i,0}^{\mathrm{NBS}}(t+k|_t)\,C(t+k|_t);\,\Big]\Big]\\ \underline{TM}_i^{\mathrm{comf}}\leq TM_i^{\mathrm{in}}(t)\leq\overline{TM}_i^{\mathrm{comf}};\\ 0\leq P_{i,l}^{\mathrm{NBS}}(t)\leq\bar{P}_i;\\ \lambda_{i,l}{=}1;\,k\in\mathbb{K};\,t\in\mathbb{T};\,i\in\mathbb{I}_0\end{cases}\tag{8}$$

$P_{i,l}^{\mathrm{NBS}}(t)$ is the feasible cooperation control plan. If there is no solution or $\lambda_{i,l}{=}0$, this AC will not cooperate in the *l-th* negotiation. In this case, let $P_{i,l}^{\mathrm{NBS}}(t){=}P_{i,l-1}^{\mathrm{NBS}}(t)$. $P_{i,l}^{\mathrm{NBS}}(t)$ is packed and sent to the cloud for the next negotiation.

### C. Cooperation Decision Model for Cloud Negotiation

In the *l-th* negotiation round, an available set is recreated: $\mathbb{I}_{t,l} = \{i, P_{i,l}^{\mathrm{NBS}}(t)|_{\zeta_{i,l}(t)=1}\}$, and $\mathbb{I}'_{t,l} = \{i, P_{i,l-1}^{\mathrm{NBS}}(t)|_{\zeta_{i,l}(t)=0}\}$. If $\zeta_{i,l}(t)=0$, the packet $P_{i,l}^{\mathrm{NBS}}(t)$ experiences a dropout or a delay, and $AC_i$ as a noncooperation player that takes the last NBS values $P_{i,l-1}^{\mathrm{NBS}}(t)$. $\mu_{i,l}(t)\in\{0,1\}$ is the cooperation decision variable. $\mu_{i,l}(t)=1$ governs the cooperation *of* $AC_i$, and $\mu_{i,l}(t)=0$ governs the noncooperation of $AC_i$. The negotiation decision model is

$$\begin{cases}\min P_l^{\mathrm{DP}}\big(t+k_l^{DP}|_t\big)\\ P_l^{\mathrm{DP}}\big(t+k_l^{DP}|_t\big)\geq P^{g'}(t+k|_t)\\ \quad+\sum_{i=1,i\in I_{t,l}}^{N}\Big[\Big(\mu_{i,l}(t)P_{i,l}^{\mathrm{NBS}}(t+k|_t)\\ \qquad+\big(1-\mu_{i,l}(t)\big)P_{i,l-1}^{\mathrm{NBS}}(t+k|_t)\Big)\Big]\\ \quad+\sum_{i=1,i\in\mathcal{I}'_{t,l}}^{N}P_{i,l-1}^{\mathrm{NBS}}(t+k|_t)\\ P_{i,l}^{\mathrm{NBS}}(t+k|_t)\in\mathbb{I}_{t,l};\,P_{i,l-1}^{\mathrm{NBS}}(t+k|_t)\in\mathbb{I}'_{t,l-1};\\ k\in\mathbb{K};\,t\in\mathbb{T};\,i\in\mathbb{I}_{t,0}\end{cases}\tag{9}$$

Where $P_l^{\mathrm{DP}}(t+k_l^{DP}|_t)$ is the DP.

*1) The Bargaining Process and Achievement of the AP:* Let $l$ be the number of bargaining steps, $l=0,1,\ldots l_{\max}$. The maximum number of bargaining steps is determined by the control duration. If $P_l^{\mathrm{DP}}(t{+}k_l^{DP}|_t){-}P_{l-1}^{\mathrm{DP}}(t{+}k_{l-1}^{DP}|_t)<0$, the peak value may decrease further. $P_l^{\mathrm{DP}}(t+k_l^{\mathrm{DP}}|_t)$ as the DP is packed and broadcast to each AC for the next cooperation. If $P_l^{\mathrm{DP}}(t+k_l^{DP}|_t)-P_{l-1}^{\mathrm{DP}}(t+k_{l-1}^{DP}|_t)<\delta$ ($\delta$ is a given error) or $P_l^{\mathrm{DP}}(t+k_l^{DP}|_t)-P_{l-1}^{\mathrm{DP}}(t+k_{l-1}^{DP}|_t)>0$, the minimum critical peak of the grid is found, and the AP is achieved. If $l=l_{\max}$, the AP is $P_{l_{\max}}^{\mathrm{DP}}(t{+}k_{l_{\max}}^{DP}|_t)$. Thus, the optimal control sequence of $AC_i$ at the AP can be written as

$$\begin{aligned}P_i^{\mathrm{AP}}(t)=&\big[\mu_{i,l}(t)P_{i,l}^{\mathrm{DP}}(t)+\big(1-\mu_{i,l}(t)\big)P_{i,l-1}^{\mathrm{DP}}(t)\big]_{i\in\mathcal{I}_{i,l}}\\&+\big[P_{i,l-1}^{\mathrm{DP}}(t)\big]_{i\in\mathcal{I}'_{i,l}}.\end{aligned}$$

According to MPC, only the first step in the resulting optimal control sequence is applied. The control packet sent to the $AC_i$ actuator is

$$\tilde{P}_i^{\mathrm{act}}(t)=ZP_i^{\mathrm{AP}}(t),\,Z=\left[1,\underbrace{0,\ldots0}_{K_T-1}\right].\tag{10}$$

*2) Feedback Compensation for the Actuator:* Considering the unreliability of the cloud and the communication channel, if $\gamma_i(t){=}\,0$ is detected, the first item of $P_{i,l}^{NBS}(t)$ is fed back to the actuator as compensation to maintain control stability and optimization. The output of the actuator is

$$\begin{aligned}P_i^{\mathrm{act}}(t)=&\gamma_i(t)\tilde{P}_i^{\mathrm{act}}(t)+(1-\gamma_i(t))ZP_{i,l}^{NBS}(t),\\Z=&\left[1,\underbrace{0,\ldots0}_{K_T-1}\right]\end{aligned}\tag{11}$$

In the next control step, the state reached at time $t{+}1$ is measured, and the above process is repeated.

To summarize the above process, the flowchart of the CEC control is given in Fig. 4.

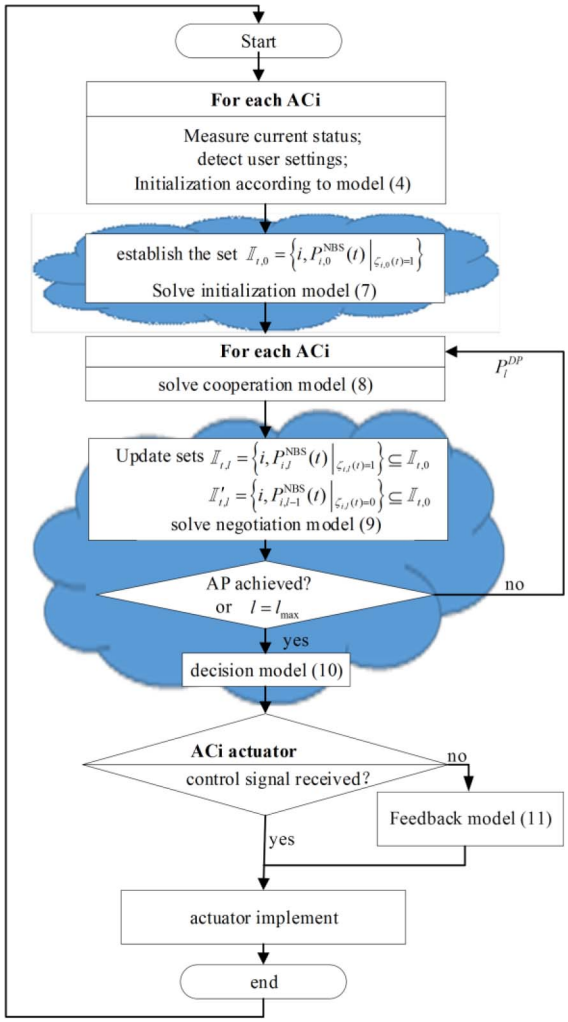


Fig. 4. Flowchart of the CEC control in one step.

### *D. Computational Complexity and Communication Overhead Analysis*

The centralized model (4) for the cloud is a nonlinear multiobjective optimization problem. The number of variables increases greatly as the number of ACs increases. For example, if $5\times10^4$ ACs participate in coordination, when the prediction horizon is 24 h (a sampling interval of 10 min and 144 control periods), there are more than 30 million variables, which is an extremely large-scale problem. Moreover, all house parameters, settings, statuses, and forecast information about the private ACs must be uploaded to the cloud for storage.

We use this example to analyze the computational complexity and communication overhead of the proposed CEC strategy. The number of calculations undertaken by the chip of each AC is as follows: model (1) has 289 variables, and model (8) has 290 variables. It can be solved by almost any solver. The number of calculations undertaken by the cloud is as follows: model (7) has only one variable, and this variable is a scalar. Model (9) is an integer linear programming (ILP) model. The number of variables is equal to the number of ACs plus 1. There are 50,001 variables in the example. Current commercial solvers (such as *LocalSolver* and *GRUOBI*) have been able to solve combinatorial optimization problems with millions of variables.

There is communication between the edged chip and the cloud. $P_{i,l}^{\mathrm{NBS}}(t)$ is uploaded by the chip to the cloud as a vector with 144 elements. $P_l^{\mathrm{DP}}(t)$, which is broadcasted by the cloud, is a scalar. The control decision $P_i^{\mathrm{act}}(t)$ is also a scalar. The cloud center only needs storage sets $\mathbb{I}_{t,l}=\{i,P_{i,l}^{\mathrm{NBS}}(t)|_{\zeta_{i,l}(t)=1}\}$ and $\mathbb{I}'_{t,l}=\{i,P_{i,l-1}^{\mathrm{NBS}}(t)|_{\zeta_{i,l}(t)=0}\}$.

TABLE I
OPERATIONAL PARAMETERS OF THE ACS

| ACi | $\alpha_i$ | $\beta_i$ | $\overline{TM_i^{\mathrm{comf}}}$ | $\underline{TM_i^{\mathrm{comf}}}$ | $TM_i^{\mathrm{comf}}$ | $\overline{P_i}$ |
|---|---|---|---|---|---|---|
| AC1 | 0.40 | -4.2 | 29 | 24 | 27 | 3 |
| AC2 | 0.30 | -3.4 | 27 | 22 | 24 | 3 |
| AC3 | 0.35 | -6.0 | 28 | 23 | 25 | 3 |
| AC4 | 0.40 | -5.0 | 28 | 22 | 24 | 3 |
| AC5 | 0.45 | -4.0 | 28 | 24 | 26 | 3 |
| AC6 | 0.32 | -3.0 | 27 | 22 | 25 | 3 |

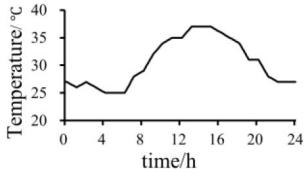


Fig. 5. Outdoor temperature.

## V. CASE STUDIES

In this section, we simulate two cases to demonstrate the feasibility and effectiveness of the proposed CEC strategy. Amazon EC2 offers a wide selection of cloud instance types with various combinations of CPUs, memory sizes, storage capacities, and networking speeds. The cases studied in this paper were analyzed on a 3rd generation Compute Optimized instance type C3.2xlarge with eight virtual CPUs, 15 GB of memory, and 160 GB of SSD storage. The simulation of the embedded chip is performed on a personal computer with an i7 2.7 GHz processor and 4 GB of random memory.

Because random disturbance and inaccurate predictions have a great influence on the result, to filter the influence, we assume that the predictions are accurate and it is undisturbed in the control process.

### *A. Case 1*

To facilitate observation, six ACs with different parameters and a simulated grid load are used for simulation. The parameters of the ACs are shown in Table I. Assume that the CPP range is 67-72 time slots, and the price is 2.5¥/kWh. The flat price is 0.8¥/kWh. The outdoor temperature is shown in Fig. 5. The grid baseload is the grid removed by the ACs, the nonresponse CPP of the ACs and the total load profile are shown in Fig. 6. The proportion of the ACs is shown in Fig. 7. The AC load accounts for approximately 20% of the total peak load. Fig. 8 shows that, if an AC responds to the

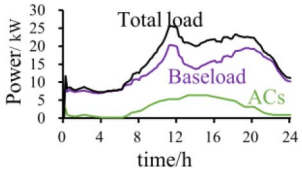


Fig. 6. Profile of non-response.

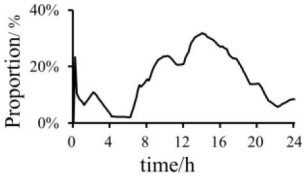


Fig. 7. Proportion of the ACs.

TABLE II
COMPARISON OF POWER PEAK CHANGES /KW (65-72 TIMESLOTS)

| response strategy | time slot | | | | | | | |
|---|---|---|---|---|---|---|---|---|
| | 65 | 66 | 67 | 68 | 69 | 70 | 71 | 72 |
| non-response to price | 23.11 | 24.17 | 25.5 | **25.57** | 25.53 | 25.43 | 25.4 | 25.07 |
| Synch-response | 22.94 | **25.70** | 23.2 | 25.05 | 25.01 | 24.91 | 24.9 | 23.08 |
| CEC strategy | 24.55 | 22.75 | 24.1 | **24.92** | 24.88 | 24.78 | 24.7 | 23.11 |
| AC1 upload packets loss | 24.45 | 22.85 | 24.1 | **24.92** | 24.88 | 24.78 | 24.7 | 23.18 |
| AC1 decision loss | 24.02 | 23.7 | 23.8 | **24.94** | 24.9 | 24.8 | 24.7 | 23.08 |

CPP dependently, the loads shift at the same time. Two peaks form in slots 66 and 73. Different control strategies and scenarios are simulated for comparison, and the results are shown in Fig. 9-Fig. 11 and Table II-Table V. For clearer observation, we simply show the 55th-83rd time slots, which include the violent fluctuation period. Fig. 9, Fig. 10, and Fig. 11 show that all the ACs cool down simultaneously in the 66th timeslot when responding to the CPP without cooperation. A critical peak appears. The peak value of 25.74 kW exceeds the peak value of 25.57 kW when there is no price response, which means that the peak value increases by 0.7% (Table II).

The CEC control strategy proposed in this paper is adopted, and the control scheduling of AC1, AC2, and AC3 is changed. The peak shifts to the 65th time slot, causing the grid peak to drop to 24.92 kW, which is 2.5% less than the non-response to price and 3.2% less than the synch-response. Moreover, the simulation results of AC1 packet $P^{\mathrm{NBS}}_{\mathrm{AC1},1}(t)$lossed or packet $P^{\mathrm{DP}}_{\mathrm{AC1},1}(t)$lossed, which shows that the cooperating player is AC2 and instead of AC6, but the peak remains at 24.92 kW. When the AC1 decision packet $\tilde{P}^{\mathrm{act}}_{\mathrm{AC1}}(t)$ drops out, the feedback compensation is the noncooperation value. The peak is 24.94 kW, which has risen slightly but is still 3.1% less than the synch-response. The results show that packet loss occurs in the feedforward channel, which changes the cooperation combination but has little effect on the peak of the grid. Packet loss occurs in the feedback channel, which has an impact on the peak of the grid, but it is very small. The electric tariff of each AC for 24 h is shown in Table III. The table shows that the tariff of the CEC strategy is the same as that of noncooperation. Table IV shows that the lowest and highest temperature does not exceed the user's limit. However, Table V shows that the objective function of the selected cooperative player is slightly increased due to the increase in the indoor temperature fluctuation.

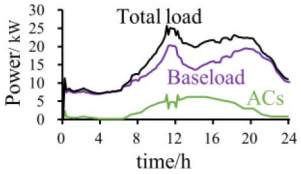


Fig. 8. ACs response to CPP.

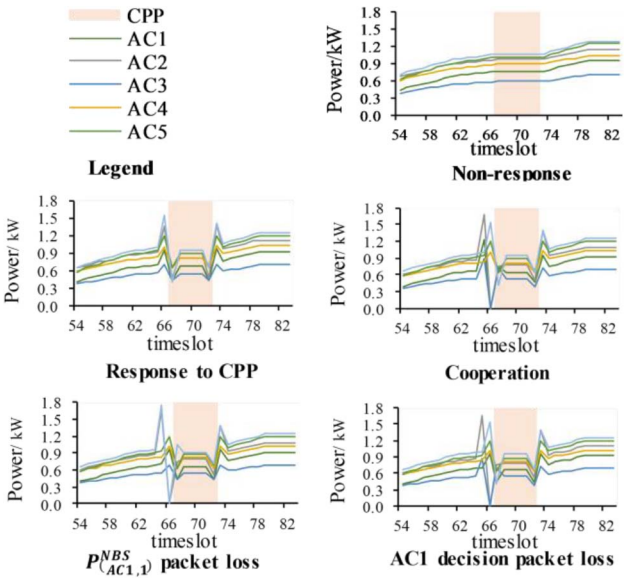


Fig. 9. Power consumption comparison.

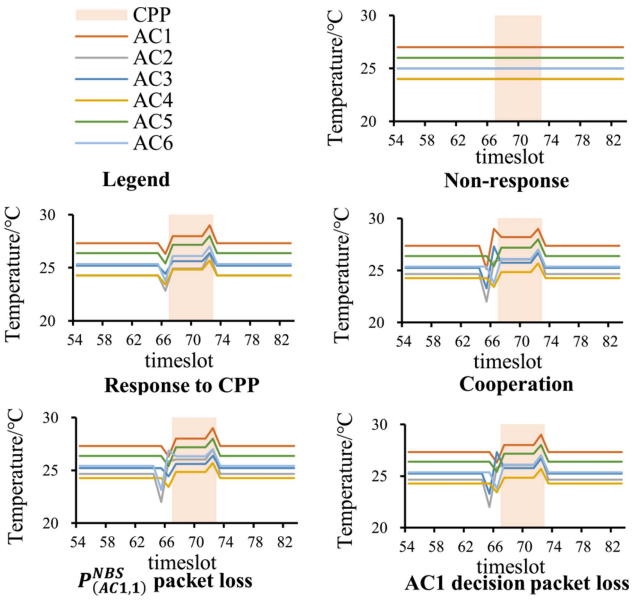


Fig. 10. Comparison of indoor temperature changes.

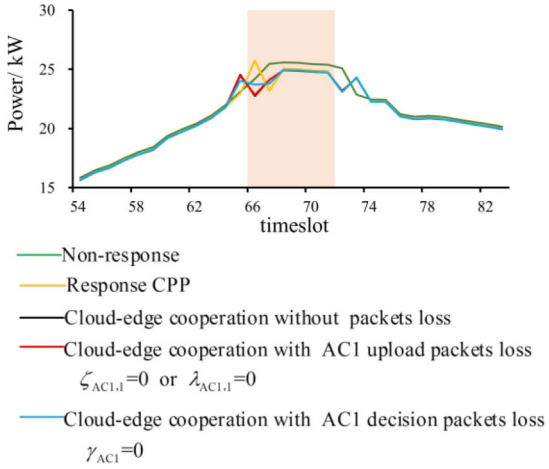


Fig. 11. Critical peak comparison.

TABLE III
COMPARISON OF ELECTRIC TARIFF (¥)

| Response strategy | AC1 | AC2 | AC3 | AC4 | AC5 | AC6 |
|---|---|---|---|---|---|---|
| Non-response to price | 8.43 | 12.88 | 7.27 | 11.66 | 11.88 | 13.31 |
| Synch-response | 7.70 | 11.93 | 6.91 | 10.99 | 10.75 | 12.11 |
| CEC strategy | 7.70 | 11.93 | 6.91 | 10.99 | 10.75 | 12.11 |
| AC1 upload packets loss | 7.70 | 11.93 | 6.91 | 10.99 | 10.75 | 12.11 |
| AC1 decision packet loss | 7.70 | 11.93 | 6.91 | 10.99 | 10.75 | 12.11 |

TABLE IV
COMPARISON OF INDOOR TEMPERATURE CHANGES BEFORE AND AFTER RESPONSE TO PRICE

| Response strategy | AC1 | AC2 | AC3 | AC4 | AC5 | AC6 |
|---|---|---|---|---|---|---|
| Non-response to price | 27.0 | 24.0 | 25.0 | 24.0 | 26.0 | 25.0 |
| | 27.0 | 24.0 | 25.0 | 24.0 | 26.0 | 25.0 |
| Synch-response CPP | 26.3 | 22.8 | 24.4 | 23.4 | 25.4 | 23.8 |
| | 29.0 | 26.4 | 26.4 | 25.7 | 28.0 | 27.0 |
| CEC strategy | 25.1 | 22.0 | 23.3 | 23.4 | 25.4 | 23.8 |
| | 29.0 | 27.0 | 26.7 | 25.7 | 28.0 | 27.0 |
| AC1 upload packets loss | 26.3 | 22.0 | 24.4 | 23.4 | 25.4 | 23.1 |
| | 29.0 | 27.0 | 26.4 | 25.7 | 28.0 | 27.0 |
| AC1 decision packet loss | 26.3 | 22.0 | 23.3 | 23.4 | 25.4 | 23.8 |
| | 29 | 27 | 26.7 | 25.7 | 28 | 27 |

Note: the green is the lowest temperature. The white is the highest temperature.

## B. Case 2

The simulation controls up to $5 \times 10^4$ distributed ACs in a region. The AC energy efficiency coefficient is randomly generated in the range of 3-5. The room thermal mass coefficient is randomly generated in the range of 0.3-0.6. The most comfortable indoor temperature is set to 26°C according to Chinese standards. The allowed indoor temperature fluctuation range is set to 24-28°C (and is user-defined). The TOU published by power utilities in the summer is listed in Table VI. The outdoor temperature based on measurements on a summer day is shown in Fig. 12. The baseload is shown in Fig. 13.

TABLE V
COMPARISON FOR THE USER' OBJECT OF MODEL (1)

| Response strategy | AC1 | AC2 | AC3 | AC4 | AC5 | AC6 |
|---|---|---|---|---|---|---|
| Non-response to price | - | - | - | - | - | - |
| Synch-response | 9.45 | 12.41 | 7.09 | 11.32 | 11.57 | 12.67 |
| CEC strategy | 9.70 | 13.18 | 7.34 | 11.32 | 11.57 | 12.67 |
| AC1 upload packets loss | 9.45 | 13.18 | 7.09 | 11.32 | 11.57 | 12.99 |
| AC1 decision packet loss | 9.45 | 13.18 | 7.34 | 11.32 | 11.57 | 12.67 |

TABLE VI
TIME-OF-USE

| | Time | Electricity price ¥/kWh |
|---|---|---|
| Valley | 23:00–07:00 | 0.38 |
| Flat | 07:00–10:00 | 0.84 |
| | 15:00–18:00 | 0.84 |
| | 21:00–23:00 | 0.84 |
| Peak | 10:00–15:00 | 1.32 |
| | 18:00–21:00 | 1.32 |

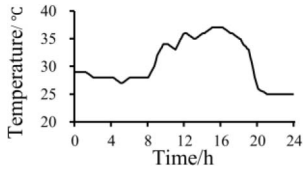


Fig. 12. Outdoor temperature.

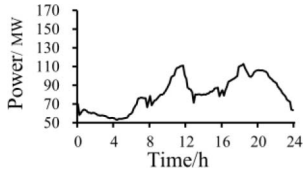


Fig. 13. Baseload of Grid

In this case, the duration of computing and uploading for each AC controller is set to 10 s, which enables the chip to have enough time to solve the NBS and the cloud to have enough time to receive the NBSs of all the ACs. The computational time to solve model (8) for one AC is 0.028 s. Obviously, this can meet the time requirements of computing and transmission. However, simulating 50,000 parallel problems is not a trivial task. A test NBS calculation of model (8) for 500 ACs takes 8.169 s. With 100 duplicates, that is, by extending the number of ACs from 500 to 50,000, the identifiers can be written, and the bijection between the models and the numbers can be determined. It can be assumed that 1 in 500 ACs have the same parameters. Therefore, the total computational time for simulating 50,000 ACs is less than 10 s. It takes 3.156 s for *LocalSolver* to solve model (9) for one bargaining process in the cloud. Model (9) is called three times to achieve the AP. The DP convergence curve is shown in Fig. 14. The load profile comparison is shown in Fig. 15.

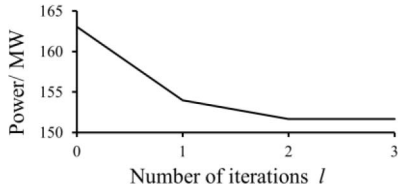


Fig. 14. The DP convergence curve.

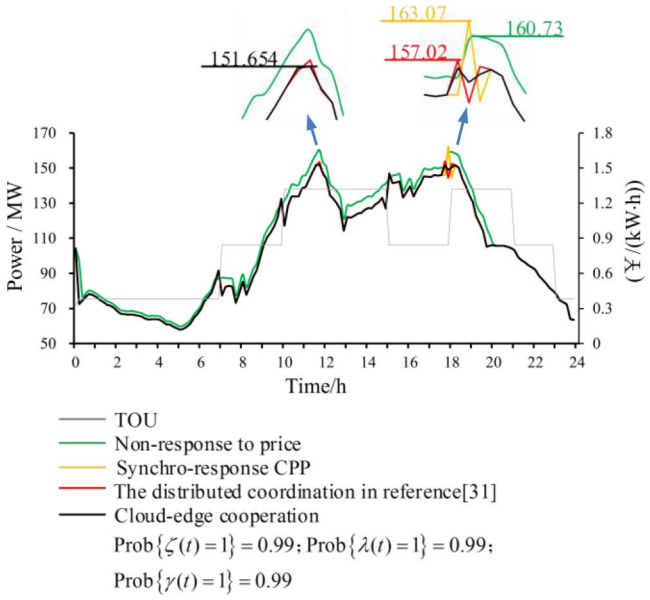


Fig. 15. Load profile comparison.

The critical peak occurs at 11:40 (the 71st control period), and the value is 160.73 MW if all ACs do not respond to the price. If all ACs respond synchronously to the price, the peak time moves from 11:40 to 17:50, and the peak value is 163.07 MW, which means that the peak value increases by 1.46% compared to the nonresponse. The distributed coordination peak value in [31] is 157.02 MW and appears at 17:40. Even better, the maximum peak after CEC is at 11:40, and the value is 151.65 MW, which is 5.99% less than the peak value of the nonresponse, 7.53% less than the synchro-response and 3.54% less than the distributed coordination.

## VI. Conclusion

This paper proposes a cloud-edge cooperative control model and strategy for the PBDR of large-scale ACs based on the IoT to reduce the critical peak of the grid and eliminate the peak rebound without dispatcher intervention. Further, a double feedback closed-loop control strategy is proposed to deal with uncertain events such as packet loss, delay, or downtime in the process of cloud-edge interactions. The following advantages are verified by simulation cases:

1. The cloud side cooperation strategy effectively reduces the peak of the power grid and eliminates the rebound peak.
2. In the case of packet loss, delay, or downtime, the strategy can still maintain control stability and the optimization objectives of the individual ACs.
3. The edge computing greatly reduces the computing complexity and storage of the cloud. The edge computing model has only 290 variables and can be solved quickly by any solver. Users do not need to upload any information other than the feasible power usage plan. Privacy is preserved.
4. The cloud model, which is an ILP model, was solved by commercial solvers quickly. The cloud platform does not receive and store any user information other than the feasible power usage plan. Data storage is less.

We believe that cloud-edge cooperation control can also be applied in more fields. We will do more in-depth research on the frequency response and other auxiliary services of DR.

## References

[1] Q. Shi, C. Chen, A. Mammoli, and F. Li, "Estimating the profile of incentive-based demand response (IBDR) by integrating technical models and social-behavioral factors," *IEEE Trans. Smart Grid*, vol. 11, no. 1, pp. 171–183, Jan. 2020.

[2] X. Yan, Y. Ozturk, Z. Hu, and Y. Song, "A review on price-driven residential demand response," *Renew. Sustain. Energy Rev.*, vol. 96, pp. 411–419, Nov. 2018.

[3] F. Shariatzadeh, P. Mandal, and A. K. Srivastava, "Demand response for sustainable energy systems: A review, application and implementation strategy," *Renew. Sustain. Energy Rev.*, vol. 45, pp. 343–350, May 2015.

[4] T. Samad, E. Koch, and P. Stluka, "Automated demand response for smart buildings and microgrids: The state of the practice and research challenges," *Proc. IEEE*, vol. 104, no. 4, pp. 726–744, Apr. 2016.

[5] W. Cui *et al.*, "Evaluation and sequential dispatch of operating reserve provided by air conditioners considering lead–lag rebound effect," *IEEE Trans. Power Syst.*, vol. 33, no. 6, pp. 6935–6950, Nov. 2018.

[6] K. McKenna and A. Keane, "Residential load modeling of price-based demand response for network impact studies," *IEEE Trans. Smart Grid*, vol. 7, no. 5, pp. 2285–2294, Sep. 2016.

[7] S. Bahrami, V. W. Wong, and J. Huang, "An online learning algorithm for demand response in smart grid," *IEEE Trans. Smart Grid*, vol. 9, no. 5, pp. 4712–4725, Sep. 2018.

[8] J. Baillieul, M. C. Caramanis, and M. D. Ilik, "Control challenges in microgrids and the role of energy-efficient buildings," *Proc. IEEE*, vol. 104, no. 4, pp. 692–696, Apr. 2016.

[9] A. Jiang and H. Wei, "A dynamic optimized model and the on-line control strategy response to uncertainty PTR for the CPS of smart air conditioning," in *Proc. Chin. Soc. Elect. Eng.*, vol. 36, 2016, pp. 1536–1543.

[10] J. H. Yoon, R. Baldick, and A. Novoselac, "Dynamic demand response controller based on real-time retail price for residential buildings," *IEEE Trans. Smart Grid*, vol. 5, no. 1, pp. 121–129, Jan. 2014.

[11] S. Bahrami, M. H. Amini, M. Shafie-khah, and J. P. Catalao, "A decentralized electricity market scheme enabling demand response deployment," *IEEE Trans. Power Syst.*, vol. 33, no. 4, pp. 4218–4227, Jul. 2018.

[12] N. H. S. Duong, P. Maille, A. K. Ram, and L. Toutain, "Decentralized demand response for temperature-constrained appliances," *IEEE Trans. Smart Grid*, vol. 10, no. 2, pp. 1826–1833, Mar. 2019.

[13] N. Mahdavi, J. H. Braslavsky, and C. Perfumo, "Mapping the effect of ambient temperature on the power demand of populations of air conditioners," *IEEE Trans. Smart Grid*, vol. 9, no. 3, pp. 1540–1550, May 2018.

[14] S. B. Chen and R. S. Cheng, "Operating reserves provision from residential users through load aggregators in smart grid: A game theoretic approach," *IEEE Trans. Smart Grid*, vol. 10, no. 2, pp. 1588–1598, Mar. 2019.

[15] R. Adhikari, M. Pipattanasomporn, and S. Rahman, "An algorithm for optimal management of aggregated HVAC power demand using smart thermostats," *Appl. Energy*, vol. 217, pp. 166–177, May 2018.

[16] H. Hui, Y. Ding, W. Liu, Y. Lin, and Y. Song, "Operating reserve evaluation of aggregated air conditioners," *Appl. Energy*, vol. 196, pp. 218–228, Jun. 2017.

[17] C. Y. Zhang, Q. Wang, J. H. Wang, P. Pinson, J. M. Morales, and J. Østergaard, "Real-time procurement strategies of a proactive distribution company with aggregator-based demand response," *IEEE Trans. Smart Grid*, vol. 9, no. 2, pp. 766–776, Mar. 2018.
[18] R. Halvgaard, L. Vandenberghe, N. K. Poulsen, H. Madsen, and J. B. Jørgensen, "Distributed model predictive control for smart energy systems," *IEEE Trans. Smart Grid*, vol. 7, no. 3, pp. 1675–1682, May 2016.
[19] E. Vrettos, F. Oldewurtel, and G. Andersson, "Robust energy-constrained frequency reserves from aggregations of commercial buildings," *IEEE Trans. Power Syst.*, vol. 31, no. 6, pp. 4272–4285, Nov. 2016.
[20] A. Schlueter, P. Geyer, and S. Cisar, "Analysis of georeferenced building data for the identification and evaluation of thermal microgrids," *Proc. IEEE*, vol. 104, no. 4, pp. 713–725, Apr. 2016.
[21] B. Celik, R. Roche, D. Bouquain, and A. Miraoui, "Decentralized neighborhood energy management with coordinated smart home energy sharing," *IEEE Trans. Smart Grid*, vol. 9, no. 6, pp. 6387–6397, Nov. 2018.
[22] J. M. Du, "An evolutionary game coordinated control approach to division of labor in multi-agent systems," *IEEE Access*, vol. 7, pp. 124295–124308, 2019.
[23] P. Zhao, S. Suryanarayanan, and M. G. Simoes, "An energy management system for building structures using a multi-agent decision-making control methodology," *IEEE Trans. Ind. Appl.*, vol. 49, no. 1, pp. 322–330, Jan./Feb. 2013.
[24] S. Weckx, R. D'Hulst, and J. Driesen, "Primary and secondary frequency support by a multi-agent demand control system," *IEEE Trans. Power Syst.*, vol. 30, no. 3, pp. 1394–1404, May 2015.
[25] S. Chouikhi, L. Merghem-Boulahia, M. Esseghir, and H. Snoussi, "A game-theoretic multi-level energy demand management for smart buildings," *IEEE Trans. Smart Grid*, vol. 10, no. 6, pp. 6768–6781, Nov. 2019.
[26] P. Srikantha and D. Kundur, "Resilient distributed real-time demand response via population games," *IEEE Trans. Smart Grid*, vol. 8, no. 6, pp. 2532–2543, Nov. 2017.
[27] K. Dehghanpour and H. Nehrir, "Real-time multiobjective microgrid power management using distributed optimization in an agent-based bargaining framework," *IEEE Trans. Smart Grid*, vol. 9, no. 6, pp. 6318–6327, Nov. 2018.
[28] A. Abiri-Jahromi and F. Bouffard, "Contingency-type reserve leveraged through aggregated thermostatically-controlled loads—Part I: Characterization and control," *IEEE Trans. Power Syst.*, vol. 31, no. 3, pp. 1972–1980, May 2016.
[29] B. Celik, R. Roche, S. Suryanarayanan, D. Bouquain, and A. Miraoui, "Electric energy management in residential areas through coordination of multiple smart homes," *Renew. Sustain. Energy Rev.*, vol. 80, pp. 260–275, Dec. 2017.
[30] W. Cui *et al.*, "Evaluation and sequential-dispatch of operating reserve provided by air conditioners considering lead–lag rebound effect," *IEEE Trans. Power Syst.*, vol. 33, no. 6, pp. 6935–6950, Nov. 2018.
[31] A. Jiang and H. Wei, "Distributed cooperation model and optimal control strategy for interaction between large-scale air conditioning and power grid based on communication," in *Proc. Chin. Soc. Elect. Eng.*, vol. 38, 2018, pp. 6276–6283.
[32] Y. Zheng, S. Li, and H. Qiu, "Networked coordination-based distributed model predictive control for large-scale system," *IEEE Trans. Control Syst. Technol.*, vol. 21, no. 3, pp. 991–998, May 2013.
[33] D. S. Callaway, "Tapping the energy storage potential in electric loads to deliver load following and regulation, with application to wind energy," *Energy Convers. Manag.*, vol. 50, pp. 1389–1400, May 2009.
[34] J. F. Nash, "The bargaining problem," *Econometrica*, vol. 18, no. 2, pp. 155–162, 1950.
[35] J. Nash, "Two-person cooperative games," *Econometrica*, vol. 21, pp. 128–140, Jan. 1953.
[36] S. Yin, X. Li, H. Gao, and O. Kaynak, "Data-based techniques focused on modern industry: An overview," *IEEE Trans. Ind. Electron.*, vol. 62, no. 1, pp. 657–667, Jan. 2015.
[37] E. F. Camacho and C. B. Alba, *Model Predictive Control*. London, U.K.: Springer, 2013.

**Aihua Jiang** received the M.S. and Ph.D. degrees in electrical engineering from Guangxi University, Nanning, China, in 1998, and 2018 respectively, where she is currently an Associate Professor with the School of Electrical Engineering. Her research interest includes the optimization of power system operation and control. In particular, she is interested in the cyber-physical system for the smart grid.

**Hua Wei** received the B.S. and M.S. degrees in electrical engineering from Guangxi University, Nanning, China, in 1981 and 1997, respectively, and the Ph.D. degree from Hiroshima University, Japan. He is currently a Professor with Guangxi University, where he is also the Director of the Institute of Power System Optimization. His research interests include power system operation and planning, particularly the application of optimization theory and cloud technology to power systems.

**Jun Deng** received the Ph.D. degree in electrical engineering from Guangxi University, Nanning, China, in 2015. He is currently a Senior Engineer with the State Grid Shaanxi Electric Power Research Institute. His research interests include unit commitment and subsynchronous oscillation.

**Hua Qin** received the Ph.D. degree from Guangxi University, China, in 2018, where he is currently a Professor of computer engineering. His research interests include machine learning, convex optimization method, and information and communications technology.